



*Research article*

## **A PSO-enhanced Gauss pseudospectral method to solve trajectory planning for autonomous underwater vehicles**

**Wenyang Gan<sup>1</sup>, Lixia Su<sup>1</sup> and Zhenzhong Chu<sup>1,2,\*</sup>**

<sup>1</sup> Logistics Engineering College, Shanghai Maritime University, Shanghai 201306, China

<sup>2</sup> School of Mechanical Engineering, University of Shanghai for Science and Technology, Shanghai 200093, China

\* **Correspondence:** Email: [zhenzhongchu@usst.edu.cn](mailto:zhenzhongchu@usst.edu.cn); Tel.: +8602155270456.

**Abstract:** A fast optimization method based on the Gauss pseudospectral method (GPM) and particle swarm optimization (PSO) is studied for trajectory optimization of obstacle-avoidance navigation of autonomous underwater vehicles (AUVs). A multi-constraint trajectory planning model is established according to the dynamic constraints, boundary constraints, and path constraints. The trajectory optimization problem is converted into a non-linear programming (NLP) problem by means of the GPM, which is solved by the sequential quadratic programming (SQP) algorithm. Aiming at the initial values dependence of the SQP algorithm, a method combining PSO pre-planning with the GPM is proposed. The pre-planned trajectory points are configured on the Legendre-Gauss (LG) points of the GPM by fitting as the initial values for the SQP calculated trajectory planning problem. After simulation analysis, the convergence speed of the optimal solution can be accelerated by using the pretreated initial values. Compared to the linear interpolation and the cubic spline interpolation, the PSO pre-planning method improves computational efficiency by 82.3% and 88.6%, which verifies the effectiveness of the PSO-GPM to solve the trajectory optimization problem.

**Keywords:** autonomous underwater vehicles; Gauss pseudospectral method; particle swarm optimization; trajectory optimization; optimal control

---

### **1. Introduction**

With the development and utilization of marine resources, the application scenarios and

requirements of autonomous underwater vehicles (AUVs) are becoming increasingly extensive. AUVs play an essential role in marine environment observation [1,2], underwater target detection [3], seabed topographic mapping [4], and other fields. As an essential tool for developing marine resources, AUVs have the advantages of substantial autonomy and controllability [5], low operational risk, and economic advantages. Facing the complex underwater environment, an effective trajectory planning method is the key to ensuring the safety of AUVs.

The motion planning of an AUV is divided into path planning and trajectory planning. The main difference between these two categories is that there is only a series of way-points in the result obtained by path planning algorithms. However, information on time corresponding to the state is also included in the solutions obtained by trajectory planning algorithms [6]. In [7], Wang et al. proposed a novel simultaneous planning and control (SPC) method, which combines an improved artificial potential field (IAPF) and model predictive control (MPC) techniques. The IAPF is used for robust and efficient tracking in a short future. The MPC is implemented to generate actual control commands for high-precision tracking. In [8], for swarm intelligent algorithms, focusing on trajectory planning of carrier aircraft on deck, an optimal control problem was first established. Transformation of control variable was conducted to guarantee enough feasible solutions, and a segmented fitness function was set to treat the constraints discriminately and make the search efficient.

Ren et al. [9] changed the traditional A\* algorithm into a dynamic measurement heuristic A\* algorithm, which improved search efficiency. Liu et al. [10] optimized the algorithm's convergence speed and solution quality by updating the pheromone-based linear regression. Chu et al. [11] introduced an ocean current disturbance function in the deep reinforcement learning algorithm, which reduced the delay time of path planning. Trajectory planning theory has been widely used in the fields of aircraft [12], robotic arms [13] and automatic driving [14]. Liu and Zhang [15] designed an iterative strategy based on the initial values generator and improved the solution efficiency. In [16], the adaptive pseudospectral method was used to solve the optimal state and control variables of fuel consumption. In [17], the GPM was used to plan the overtaking trajectory on the curve and realized the tracking control of the trajectory.

The trajectory planning method can plan the speed and acceleration of the AUV to meet the requirements of smoothness and speed controllability. The essence of the trajectory optimization problem is the optimal control problem, which can be solved by indirect and direct methods [18]. The indirect method mainly converts the first-order necessary condition of the optimal control problem into a Hamiltonian boundary value problem, and it obtains an accurate analytical solution by solving the Hamiltonian boundary value problem. In [19], a symplectic pseudospectral method based on the dual variational principle and the quasilinearization method was proposed and was successfully applied to solve nonlinear optimal control problems with inequality constraints. Wang et al. [20] proposed an iterative framework to solve optimal control for nonlinear proportional state-delay systems. Due to the benefit of the successive convexification technique and the multi-interval pseudospectral method, initial guess on costate variables is avoided and converged solutions can be obtained with an exponential convergence rate. The disadvantage of the indirect method is that it requires the derivation of the Hamiltonian function for solution. In addition, there is no exact analytical solution for nonlinear complex control problems, so it is difficult to solve them using indirect methods.

The direct method to solve the trajectory planning problem is to transform it into a NLP problem by discretization [21]. Then, the optimal solution of the NLP problem is solved according to the KKT (Karush-Kuhn-Tucker) condition. The GPM constructs a sparse constrained Jacobian matrix through

the placement of discrete points [22]. The GPM can obtain higher accuracy with fewer collocation points, and it has the advantage of fast solution speed, which is conducive to solving optimal control problems. In [23], the Legendre-Gauss method is improved, with higher computational efficiency and accuracy in solving optimal control problems. In [24], the application of GPM in the flight phase of aircraft and rockets was discussed. Ma et al. [25] proposed a path-planning method for unmanned surface vehicles (USVs) based on the rapid Gauss pseudospectral method (RGPM). This method can plan a globally time-optimal path in a complex marine environment, discretize the continuous-time optimal control path planning problem into a nonlinear programming problem, and solve and optimize the nonlinear programming problem to reduce computational costs. Simulation experiments verify the effectiveness of the path-planning method.

For small-scale dense problems, the SQP algorithm has the advantages of fast convergence speed and high accuracy when solving NLP problems. However, the SQP algorithm is sensitive to initial values. When calculating large-scale NLP problems, the dependence on initial values increases, and it is easy to fall into local optimization [26]. In order to solve the initial values dependency of the SQP algorithm, this paper proposes a method that combines the PSO algorithm and the GPM. The path pre-planning of the PSO algorithm and discretization of the GPM provide initial values reference for the SQP algorithm to solve NLP problems.

The research in this paper includes the following aspects. First, a multi-constrained trajectory optimization model is built with the shortest sailing time as the optimization objective. The kinematic model, boundary constraints, and path constraints are established. The trajectory obtained can avoid collision with obstacles. Second, combined with the dynamic characteristics of the AUV during navigation, the mathematical model of the AUV trajectory planning is improved by introducing dynamic constraints. The navigation path obtained by the solution meets the actual requirements, and the change of control variables during the navigation process is more intuitive and traceable. Finally, the PSO is used to solve the path points quickly. The pre planned path is fitted, and the trajectory points are allocated to the LG points of the GPM, which are used as the initial values of the SQP algorithm and are iterated. The search cost is reduced, and the calculation speed is improved.

The main structure of this paper is as follows: Section 2 introduces the AUV trajectory planning problem, establishes the AUV motion model, and describes the AUV constraints and optimal control problems. Section 3 describes the principles and processes of the GPM and the PSO for trajectory planning. Section 4 compares three different strategies for initial value generation by simulation calculation and verifies the validity of the PSO-GPM in solving the trajectory planning problem. Section 5 summarizes the results of this study.

## 2. Model description

The trajectory planning problem of an AUV can be described as aiming at the shortest sailing time, searching for appropriate state variables values and control variables values so that the AUV can avoid obstacles from the beginning to the end. The problems to be solved include the following three points: (1) The process from starting position to the target position of the AUV can be realized. (2) The AUV can avoid all obstacles and navigate safely during the process. (3) The AUV can navigate with an optimum or approximately optimum trajectory.

## 2.1. Motion model

The motion of the AUV is generally 6 degrees of freedom and can be decoupled into horizontal and vertical motion. Only the horizontal motion of the AUV is discussed in this paper. The mathematical model of the AUV mainly includes the kinematic model and the dynamic model. The kinematic model mainly describes the relationship between position, speed, acceleration, and time. The dynamic model considers the quality and force of the AUV and mainly analyses the motion characteristics of the robot after being stressed.

In practical applications, two directional thrusters control the movement of the AUV in three degrees of freedom: forward and backward, lateral displacement, and rotation. The distribution positions are shown in Figure 1(a).

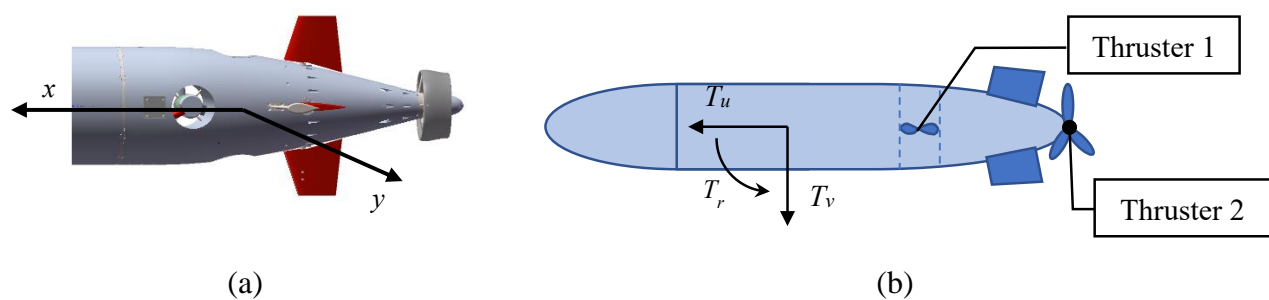


**Figure 1.** The schematic diagram of the AUV motion control. (a) The AUV thruster distribution diagram; (b) The thrust and torque diagram of AUV.

Thrusters in the  $x$  and  $y$  directions are arranged at the tail of the AUV, respectively, responsible for the forward and lateral movement of the AUV as shown in Figure 1(b). Thruster 1 generates thrust  $T_u$  in the  $x$  direction, and Thruster 2 generates thrust  $T_v$  in the  $y$  direction. The torque formed by  $T_u$  and  $T_v$  changes the navigation direction of the AUV.

The kinematic model of the AUV in the horizontal plane of motion can be expressed as follows:

$$\begin{cases} \dot{p}_x = v_x \cdot \cos \psi - v_y \cdot \sin \psi, \\ \dot{p}_y = v_x \cdot \sin \psi + v_y \cdot \cos \psi, \\ \dot{\psi} = r_z, \end{cases} \quad (1)$$

where  $p_x$ ,  $p_y$  and  $\psi$  represent the position and the direction angle of an AUV in a fixed coordinate system;  $v_x$ ,  $v_y$  and  $r_z$  represent the velocity and the angular velocity of an AUV in a moving coordinate system.

The dynamic equations of an AUV in the horizontal motion plane are expressed as follows [27]:

$$\begin{cases} M_u \dot{v}_x = M_v v_y r_z - (X_u + X_{|u|u} \cdot |v_x|) \cdot v_x + T_u \\ M_v \dot{v}_y = -M_u v_x r_z - (Y_v + Y_{|v|v} \cdot |v_y|) \cdot v_y + T_v \\ M_r \dot{r}_z = (M_u - M_v) \cdot v_x v_y - (N_r + N_{|r|r} \cdot |r_z|) \cdot r_z + T_r \end{cases} \quad (2)$$

$$\begin{cases} M_u = m - X_{\dot{u}} \\ M_v = m - Y_{\dot{v}}, \\ M_r = I_z - N_{\dot{r}} \end{cases} \quad (3)$$

where  $m$  is the mass of the AUV;  $I_z$  is the moment of inertia;  $(v_x, v_y, r_z)^T$  is the velocity vector;  $X(\cdot)$ ,  $Y(\cdot)$ , and  $N(\cdot)$  are the hydrodynamic coefficients; and  $T = (T_u, T_v, T_r)^T$  is the system input consisting of thrust and thrust torque.

## 2.2. Path constraints

Path constraints are the constraints for the AUV to avoid obstacles and navigate in a feasible area. Path constraints must satisfy the requirement that no collisions occur during the voyage. Describing the constraints accurately between obstacles and the AUV is the key to obtaining the safe trajectory. The mathematical abstraction of the AUV and obstacles can be simplified to circles or rectangles. Considering the severe consequences of collisions between the AUV and obstacles, the outline of the AUV and obstacles should be accurately described when establishing path constraints. The kinematic model of the AUV is shown in Figure 1.

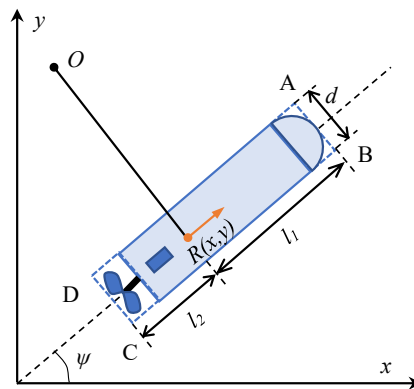


**Figure 2.** The kinematic model of the AUV.

$R(x, y)$  is the center of gravity of the AUV;  $O$  is the center of the circle for changing direction;  $l_1 = 0.8$  m and  $l_2 = 0.2$  m respectively represent the distance between  $R(x, y)$  and the front and rear edges of the AUV;  $d = 0.2$  m is the width of the AUV;  $\psi$  is the heading angle of the AUV;  $A$ ,  $B$ ,  $C$  and  $D$  are the vertices of the simplified contour of the AUV; the vertex coordinates of the AUV are represented as follows according to the geometric relationship:

$$\begin{cases} [Ax(t), Ay(t)] = [p_x(t) + l_1 \cos \psi(t) - \frac{d}{2} \sin \psi(t), p_y(t) + l_1 \sin \psi(t) + \frac{d}{2} \cos \psi(t)], \\ [Bx(t), By(t)] = [p_x(t) + l_1 \cos \psi(t) + \frac{d}{2} \sin \psi(t), p_y(t) + l_1 \sin \psi(t) - \frac{d}{2} \cos \psi(t)], \\ [Cx(t), Cy(t)] = [p_x(t) - l_2 \cos \psi(t) + \frac{d}{2} \sin \psi(t), p_y(t) - l_2 \sin \psi(t) - \frac{d}{2} \cos \psi(t)], \\ [Dx(t), Dy(t)] = [p_x(t) - l_2 \cos \psi(t) - \frac{d}{2} \sin \psi(t), p_y(t) - l_2 \sin \psi(t) + \frac{d}{2} \cos \psi(t)]. \end{cases} \quad (4)$$

The obstacle simulation method based on P-Norm criterion can express the position and shape information of obstacles in the form of functions. The form of path constraints is concise and unified, and the mathematical expression of obstacles can be flexibly adjusted to meet the formal requirements for constraint conditions in trajectory planning problems.

The P-criterion function can be expressed as

$$h(o_x, o_y) = \left( \left| \frac{o_x - a}{r_x} \right|^p + \left| \frac{o_y - b}{r_y} \right|^p \right)^{1/p} - 1, \quad p = 1, 2, 3, \dots \quad (5)$$

where  $r_x$  and  $r_y$  represent the scale coefficients in the  $x$  and  $y$  directions;  $(a, b)$  represents the center position of the graph. When  $h(o_x, o_y) = 0$ , different  $p$  values represent different graphical boundaries.

In this paper,  $P = 2$  and  $P = 6$  are selected to represent the shapes of the obstacles with a circle and an approximate rectangle. The relationship between the trajectory points of the AUV and the position of the obstacles can be expressed as

$$h_i[Ax(t), Ay(t)] = \left( \left| \frac{Ax(t) - a_i}{r_{xi}} \right|^{p_i} + \left| \frac{Ay(t) - b_i}{r_{yi}} \right|^{p_i} \right)^{1/p_i} - 1, \quad i = 1, 2, 3, 4, \quad (6)$$

where  $i$  represents the  $i$ -th obstacle. The expression of points B, C and D is consistent with Eq 6. Any point where  $h(o_x, o_y) = 0$  is located on the boundary of the obstacle. Accordingly, to achieve obstacle avoidance navigation of the AUV, it is necessary to ensure that the trajectory points of the AUV are located outside the obstacle, that is, to ensure that  $h(o_x, o_y) > 0$ .

### 2.3. Boundary constraints

In order to reach the target point safely and accurately, the AUV trajectory needs to satisfy the control and boundary constraints. The control constraints include the propeller's thrust and torque constraints, which can be expressed as follows:

$$T_{u\min} \leq T_u \leq T_{u\max}, \quad T_{v\min} \leq T_v \leq T_{v\max}, \quad T_{r\min} \leq T_r \leq T_{r\max}. \quad (7)$$

State variable constraints include position, speed, and angle constraints and can be expressed as:

$$\begin{cases} p_{x\min} \leq p_x \leq p_{x\max}, & p_{y\min} \leq p_y \leq p_{y\max}, & \psi_{\min} \leq \psi \leq \psi_{\max}, \\ v_{x\min} \leq v_x \leq v_{x\max}, & v_{y\min} \leq v_y \leq v_{y\max}, & r_{z\min} \leq r_z \leq r_{z\max}. \end{cases} \quad (8)$$

Boundary constraints include initial and terminal constraints, which correspond to the initial and terminal states of the AUV during navigation as follows:

$$\begin{cases} p_x(t_0) = p_{x0}, & p_y(t_0) = p_{y0}, & \psi(t_0) = \psi_0, \\ v_x(t_0) = v_{x0}, & v_y(t_0) = v_{y0}, & r_z(t_0) = r_{z0}. \end{cases} \quad (9)$$

$$\begin{cases} p_x(t_f) = p_{xf}, & p_y(t_f) = p_{yf}, & \psi(t_f) = \psi_f, \\ v_x(t_f) = v_{xf}, & v_y(t_f) = v_{yf}, & r_z(t_f) = r_{zf}. \end{cases} \quad (10)$$

#### 2.4. Optimal control problem

The trajectory optimization goal of the AUV is to find the trajectory with the optimal values of the control variables and satisfy the constraints by setting the objective function. The optimal control problem can be described as finding control variables  $u(t) \in R^m$  and system state variables  $x(t) \in R^n$ , minimizing performance indicators, and satisfying dynamic, path and boundary constraints.

$$J = \Phi[x(t_0), t_0, x(t_f), t_f] + \int_{t_0}^{t_f} L[x(t), u(t), t] dt \quad (11)$$

$$s.t. \begin{cases} \dot{x} = f[x(t), u(t), t], & t \in [t_0, t_f], \\ C[x(t), u(t), t] \leq 0, & t \in [t_0, t_f], \\ \phi[x(t_0), t_0, x(t_f), t_f] = 0, \end{cases} \quad (12)$$

where  $u$  represents the control variable of the system, and  $x$  represents the state variable;  $t_0$  and  $t_f$  represent the initial and final time values, respectively, and can be set as free variables;  $\Phi$  represents the Mayer form of the objective function;  $L$  represents the Lagrange form of the objective function;  $C$  represents the path constraint function;  $\phi$  represents the boundary constraint function.

In the above formula, the function satisfies the following definition range and value range.

$$\begin{aligned} \Phi &: R^n \times R \times R^n \times R \rightarrow R \\ L &: R^n \times R^m \times R \rightarrow R \\ f &: R^n \times R^m \times R \rightarrow R^n \\ \phi &: R^n \times R \times R^n \times R \rightarrow R^q \\ C &: R^n \times R^m \times R \rightarrow R^c \end{aligned} \quad (13)$$

### 3. Motion trajectory planning

GPM is a collocation method which discretizes state and control variables at a series of Legendre-Gauss (LG) points. Lagrange polynomials are used for global fitting to approximate the trajectories of state and control variables. Therefore, the optimal control problem in continuous space is transformed into a non-linear programming problem.

#### 3.1. Conversion of the optimal control problem

Since the collocation points of the GPM are all distributed in the region  $[-1, 1]$ , a time variable  $\tau \in [-1, 1]$  is introduced to discretize the time  $t \in [t_0, t_f]$  of the optimal control problem to  $[-1, 1]$ . The transformation form is as follows.

$$\tau = \frac{2t}{t_f - t_0} - \frac{t_f + t_0}{t_f - t_0} \quad (14)$$

NLG points and initial time  $\tau_0 = -1$  are selected as collocation points. The state and control variables are approximated by Lagrange interpolation polynomial and discretized into the following equation.

$$\begin{aligned} x(\tau) &\approx X(\tau) = \sum_{i=0}^N L_i(\tau) x(\tau_i) \\ u(\tau) &\approx U(\tau) = \sum_{i=1}^N L_i(\tau) U(\tau_i) \end{aligned} \quad (15)$$

where the interpolation basis function  $L_i(\tau) (i=0,1,2,\dots,N)$  is defined as  $L_i(\tau) = \prod_{j=0, j \neq i}^N \frac{\tau - \tau_j}{\tau_i - \tau_j}$  and  $L_i(\tau) (i=1,2,\dots,N)$  is defined as  $L_i(\tau) = \prod_{j=1, j \neq i}^N \frac{\tau - \tau_j}{\tau_i - \tau_j}$ .

For the integration of the dynamic differential equation on the interval  $[-1, 1]$ , the following equation can be obtained:

$$x(\tau_f) - x(\tau_0) = \frac{t_f - t_0}{2} \int_{-1}^1 f[x(\tau), u(\tau), \tau] d\tau \quad (16)$$

The state variables in Eq (15) are differentiated as follows:

$$\dot{x}(\tau_k) \approx \dot{X}(\tau_k) = \sum_{i=0}^N \dot{L}_i(\tau_k) X(\tau_i) = \sum_{i=0}^N D_{ki} X(\tau_i) \quad (17)$$

The differential of the Lagrange polynomial at LG points can be determined by off-line calculation of differential approximation matrix  $D \in R^{N \times (N+1)}$ .

In the discretization the terminal state is approximated by Gauss integration.

$$X_f = X_0 + \frac{t_f - t_0}{2} \sum_{k=1}^N \omega_k f(X(\tau_k), U(\tau_k), \tau_k, t_0, t_f) \quad (18)$$

where  $\tau_k (1,2,\dots,N)$  is the LG point, and  $\omega_k = \int_{-1}^1 L_i(\tau) d\tau$  is the Gauss weight.

The dynamic constraints of the optimal control problem are converted into algebraic constraints utilizing a differential approximation matrix, and the integral form of the state equation is obtained as follows:

$$\sum_{i=0}^N D_{ki} X(\tau_i) - \frac{t_f - t_0}{2} f[X(\tau_k), U(\tau_k), \tau_k, t_0, t_f] = 0 \quad (19)$$

### 3.2. Parameter optimization

Based on the above numerical approximation method, the continuous trajectory optimization problem is discretized and transformed into a non-linear programming problem, which can be solved by the SQP to obtain an approximate solution of the optimal control problem [28].

The selection of initial values is the key to realizing real-time or fast calculation. The quality of



initial values directly affects the time of solving optimization problems. Initial values with poor quality will increase the calculation cost and result in the optimization problem not undergoing convergence. PSO, as a typical artificial intelligence algorithm, has the advantages of easy realization and fast convergence and is widely used to solve path planning problems [29]. Compared with the standard collocation method, the GPM can obtain higher solution accuracy with fewer nodes and has a faster convergence speed [30]. By combining the advantages of the two methods, the efficiency and accuracy of solving trajectory optimization problems are improved.

The PSO aims to search for the best solution by iteration from a group of stochastic solutions. During the iteration, the individual learns information from the individual and group extremes and constantly updates its speed  $v_i$  and position  $x_i$  according to Eqs (20) and (21).

$$v_i^{t+1} = \omega v_i^t + c_1 r_1 (p_i^t - x_i^t) + c_2 r_2 (p_g^t - x_i^t) \quad (20)$$

$$x_i^{t+1} = x_i^t + v_i^{t+1} \quad (21)$$

where  $\omega$  is the inertia weight;  $c_1$  and  $c_2$  are the two learning factors, and  $r$  is a random number between (0,1);  $x_i^t$  is the position of the  $i$ -th particle at the  $t$ -th iteration;  $v_i^t$  is the velocity of the  $i$ -th particle at the  $t$ -th iteration;  $p_g$  is the Group optimal value.

When the PSO is used to solve path planning problems, the objective function is usually the shortest path. The penalty functions are set according to the constraints, and the equality and inequality constraints are weighted to convert the constrained optimization problems into unconstrained optimization problems. The fitness function of PSO includes the objective function and penalty function. If the constraints are met, the penalty function is set to 0. The particles are randomly placed in the feasible region to search, and the speed and position of the particles are changed by Eqs (20) and (21) to find the solution with the lowest fitness function. Finally, the results of path planning are obtained.

The PSO has a robust global searching ability and fast early convergence, and it is suitable for global path planning. However, it ignores the kinematic characteristics of the AUV when solving path planning problems, and the result only has position information. The trajectory planning method based on the GPM can calculate the optimum value of the state and control variables, including time information, by solving the dynamic constraints of the AUV. The information on speed and angular velocity can be directly used as the reference command of the control system. However, when solving NLP problems converted from the GPM, the SQP algorithm is sensitive to the initial values involved in the iterative calculation. The solution process depends on the selection of initial values. Combining the speed of the PSO with the accuracy of the GPM, the initial values can be optimized, and the computational efficiency of the algorithm can be improved. The PSO is used to pre-plan the path and converge the path around the optimal solution to provide initial values reference for the SQP algorithm. The pre-planned trajectory is fitted by the cubic spline interpolation so that the initial values are distributed at LG points. Fitted trajectory points are used as guessing values to improve the speed of the solution.

#### 4. Simulation analysis

Set the navigation area of the AUV to a square two-dimensional plane of 25 m  $\times$  25 m, and set the start and end points of the AUV to point (0 m, 0 m) and point (25 m, 25 m). The objective function  $J = t_f$  for AUV trajectory optimization is set to minimize navigation time. The state variables and control

variables are discretized at 50 LG points. The boundary and constraint values of state variables are shown in Table 1, and control variable constraints are shown in Table 2.

**Table 1.** State variables constraint values.

State Variables	Starting Values	Terminal Values	Minimum Values	Maximum Values
$p_x/m$	0	25	0	30
$p_y/m$	0	25	0	30
$\psi/rad$	$\pi/4$	$\pi/4$	$-\pi$	$\pi$
$v_x(m/s)$	0	0	-1	1
$v_y(m/s)$	0	0	-1	1
$r_z(rad/s)$	0	0	$-\pi/6$	$\pi/6$

**Table 2.** Control variables constraint values.

Control Variables	$T_u$	$T_v$	$T_r$
[min, max]	[-53, 74]/N	[-53, 74]/N	[-53, 74]/(N·m)

The obstacle parameters in the navigation environment are shown in Table 3, which contains four obstacles. The relevant parameters in the dynamic constraints are shown in Table 4.

**Table 3.** Parameters related to dynamic constraints.

Name	Value	Name	Value	Name	Value
$X_{\dot{u}}$	-30 kg	$X_u$	-70 kg/s	$X_{ u  \cdot u}$	-100 kg/m
$Y_{\dot{v}}$	-80 kg	$Y_v$	-100 kg/s	$Y_{ v  \cdot v}$	-200 kg/m
$N_{\dot{r}}$	-30 kg·m <sup>2</sup>	$N_r$	-50 kg·m/s	$N_{ r  \cdot r}$	-100 kg/m
$I_z$	50 kg·m <sup>2</sup>	$m$	185 kg		

**Table 4.** Obstacle parameters.

Obstacle	Center coordinates	Length/m	Width/m
1	(5 m,5 m)	2	2
2	(8 m,13 m)	8	4
3	(18 m,12 m)	4	8
4	(20 m,20 m)	2	2

For the GPM without pre-planned path points, the initial values are selected by the cubic spline interpolation between the start point and the end point. The results of trajectory optimization obtained by simulation are shown in Figure 3.

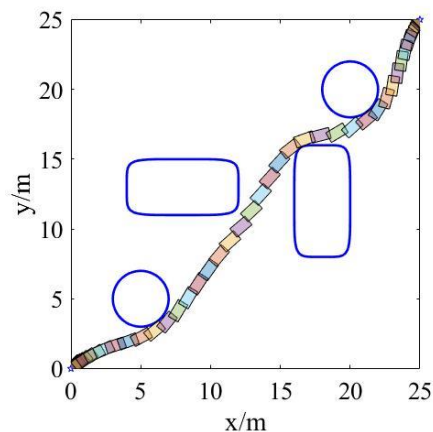


**Figure 3.** The diagram of trajectory planning results with the cubic spline interpolation.

As can be seen from Figure 3, the planned trajectory starts from the starting point (0,0). The AUV adjusts its steering angle as it approaches obstacle 1. After bypassing obstacle 1, it navigates in a straight line to the vicinity of obstacle 2 and obstacle 3. To avoid collisions, the AUV adjusts its course, traversing between obstacle 3 and obstacle 4 and navigating to the destination (25, 25).

The navigation time of the AUV is 72.742 s, and the calculation time is 92.664 s. The trajectory tends to be smooth, and the AUV can avoid collision with obstacles during navigation. The optimal trajectory satisfying the path constraints is obtained. The chart below shows the control variables and speed curves during the navigation.

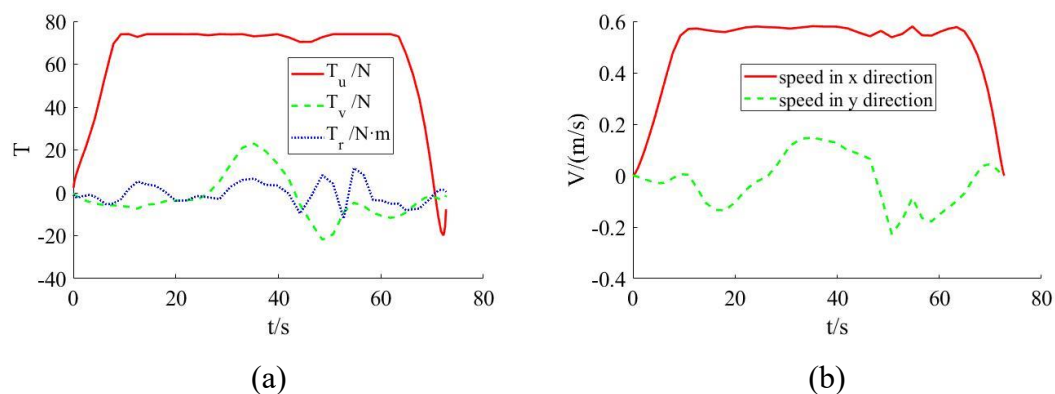


**Figure 4.** The diagram of variable values variation with the cubic spline interpolation. (a) The curve of change for control variable; (b) The curve of change in navigation speed.

Figure 4(a) shows the variation curves of control variables  $T_u$ ,  $T_v$  and  $T_r$ . It can be seen that  $T_u$ ,  $T_v$  and  $T_r$  meet the control constraints during the whole navigation. When the AUV passes obstacle 1, the torque generated by  $T_u$  and  $T_v$  causes the AUV to turn, bypass obstacle 1, and continue sailing. During the navigation time interval of [35–60 s], due to the path constraints imposed by obstacles on the AUV, the control variable  $T_v$  changes its size and direction, ensuring that the AUV can safely navigate between obstacle 3 and obstacle 4. The trend of AUV speed change is similar to that of the control variable  $T_u$ .

For the GPM without pre-planned path points, the initial values are selected by the linear interpolation between the start point and the end point. The results of trajectory optimization obtained by simulation are shown in Figure 5.

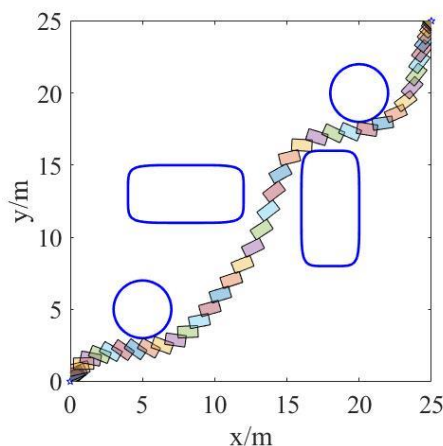


**Figure 5.** The diagram of trajectory planning results with the linear interpolation.

As can be seen from the trajectory of the AUV in Figure 5, the trajectory meets the requirements for obstacle avoidance. However, during navigation, the AUV's heading angle deviates. When the AUV is not close to an obstacle, the heading angle has undergone significant deflection, which is not conducive to the safety of the AUV navigation. The navigation time of the AUV is 67.974 s, and the calculation time is 144.173 s. The chart below shows the control variables and speed curves during the navigation.

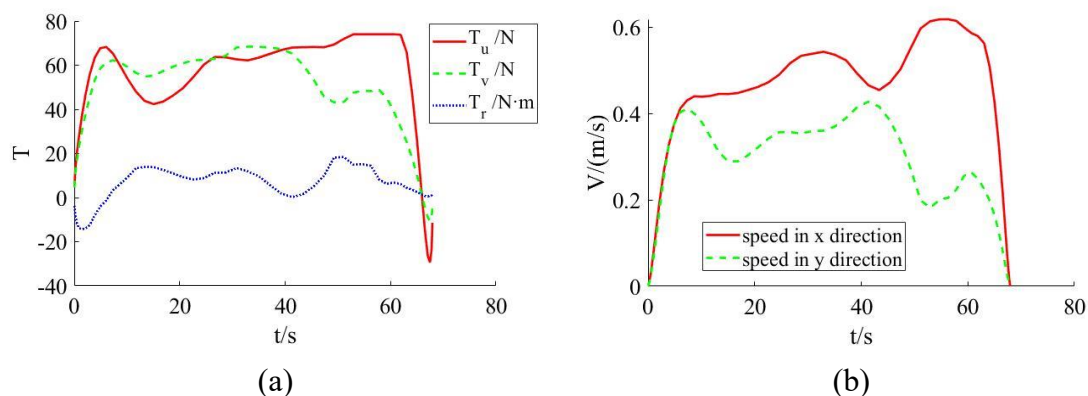


**Figure 6.** The diagram of variable values variation with the linear interpolation. (a) The curve of change for control variable; (b) The curve of change in navigation speed.

Combining the trajectory diagram in Figure 5, it can be concluded that the change in heading angle is related to the increase in the control variable values  $T$ . In Figure 6, the values of  $T$  in the  $x$  direction and the  $y$  direction are similar, and the torque generated by the two drives the AUV to change course. As a result, the AUV in Figure 5 significantly deviates from its heading when passing through obstacles.

In the same simulation environment, the PSO is introduced to pre-plan the navigation path of the AUV. The cubic spline interpolation is used to fit the pre-planned path points, and the obtained initial values are substituted for the problem of trajectory planning to solve. The results of trajectory optimization are shown in Figure 7.

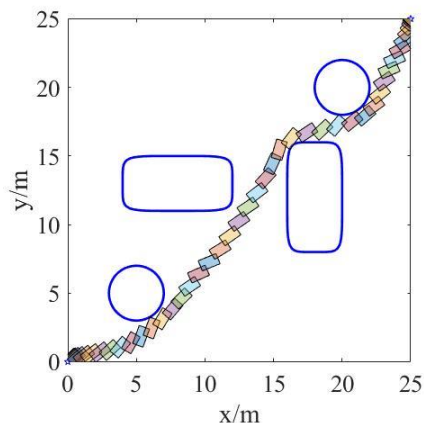


**Figure 7.** The diagram of trajectory planning results with the PSO.

The trajectory in Figure 7 satisfies the path and boundary constraints. During the voyage, there is no collision with obstacles. When the AUV passes obstacle 1, it adjusts the navigation direction to avoid collision with the obstacle. In the narrow area between obstacle 3 and obstacle 4, the AUV can also pass safely. The navigation time of the AUV is 63.507 s, and the simulation calculation time is 16.377 s. The calculation time of pre-planned path points using the PSO is 12.764 s, and the solution time after substituting pre-planned path points as initial values into the SQP is 3.613 s. After the PSO is used for pre-planning, the changes in control and state variables of the AUV are shown in Figure 8.

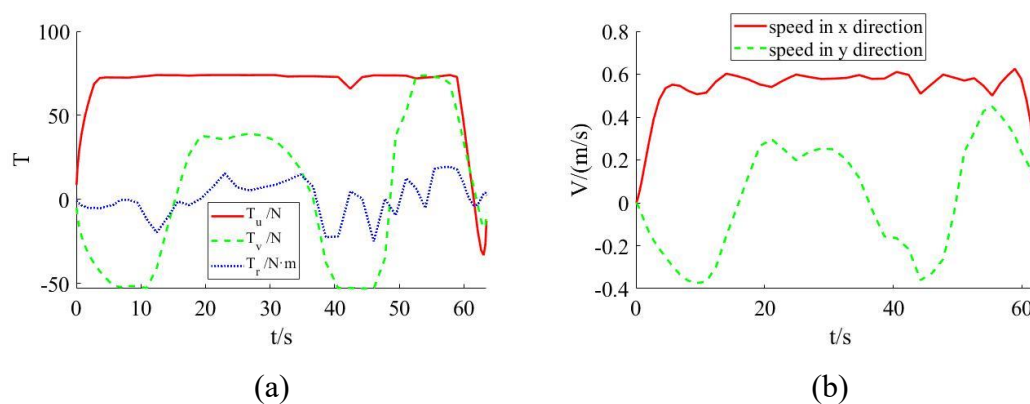


**Figure 8.** The diagram of variable values variation with PSO. (a) The control variables curve after pre-planning; (b) The speed curve after pre-planning.

In Figure 8(a),  $T_u$  drives the AUV within the restraint range with the upper thrust limit. The control variables  $T_u$ ,  $T_v$  and  $T_r$  meet the restraint requirements. During the navigation, the fluctuation of the control variable  $T_u$  is relatively small, whereas the fluctuation of  $T_v$  is relatively large. The torque generated by  $T_u$  and  $T_v$  causes the AUV's navigation direction to change.

In the above scenarios, the simulation environment is the same, and the shortest navigation time is the objective function of the trajectory optimization problem. The optimal control problem is transformed into a NLP problem by the GPM, and the optimal trajectory can be obtained quickly. The simulation results show that the optimal solution for trajectory optimization can be obtained by the GPM, and the results of trajectory planning satisfy the path constraints. At the same time, the AUV

meets the requirements for obstacle avoidance during navigation.

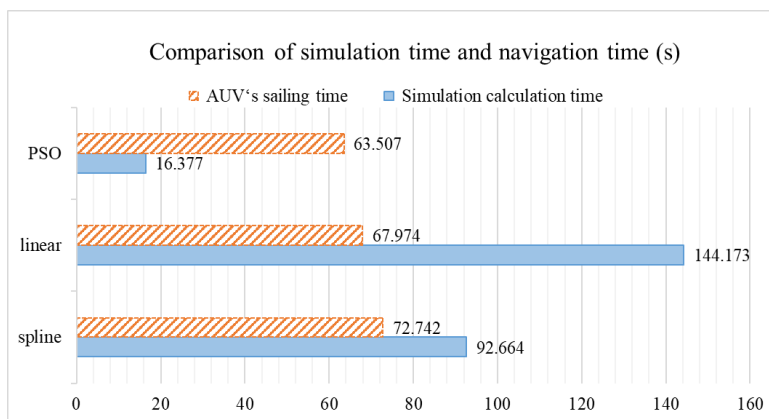


**Figure 9.** Comparison diagram of simulation time and navigation time.

Comparing the calculation times of three scenarios, it can be seen that when the PSO is used for pre-planning, a collision-free path can be quickly planned in 13 s. The pre-planned path points are fitted and assigned to the GPM as the initial values. The pre-planned trajectory is located near the optimal solution, which reduces the amount of global calculation and significantly improves the calculation speed. In Figure 9, it can be seen that the shortest sailing time is the PSO, and the shortest simulation calculation time is the PSO. After pre planning of the PSO algorithm, the SQP has significantly less time to solve trajectory optimization problems. Compared to the linear method and the spline method, the calculation efficiency by using the PSO pre-planning method is improved by 82.3 and 88.6%.

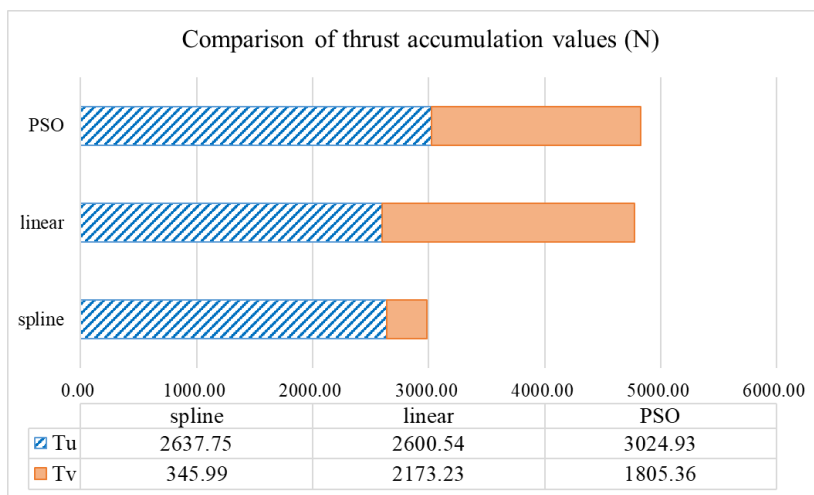


**Figure 10.** Comparison diagram of thrust accumulation values.

The thrust accumulation values reflect the demand for control during AUV navigation, which to some extent determines the AUV's navigation distance. In Figure 10, the thrust accumulation value of the PSO is the largest, and the thrust accumulation value of the spline is the smallest. Therefore, it is judged that the output of the PSO method control variables needs to be adjusted while the calculation time is optimized in order to achieve the goal of control optimization.

## 5. Conclusions

This paper takes AUV trajectory optimization as the research background and proposes the PSO method for path pre-planning to solve the initial value dependence problem of the SQP. The pre-planned path points are used as the initial values of the SQP. The combination of the PSO global search speed and the accuracy of the GPM can improve the optimum of trajectory planning. The simulation results show that the method of combining PSO and GPM reduces the calculation cost and can quickly calculate the convergent solution of the trajectory optimization problem which provides a reference for online real-time trajectory planning. The pre-planning of the PSO reduces the initial value dependency of the SQP algorithm in solving NLP problems, and it improves computational efficiency by 82.3 and 88.6% compared to the linear interpolation and the cubic spline interpolation.

The existing research results in this paper are limited to known feasible areas and the location of obstacles, and only representative obstacle models have been selected. The simulation results show that the solution results of the proposed method meet the requirements for safe navigation of the AUV. However, the selection method of LG points is relatively traditional, and the accuracy and local convergence of the solution needs to be improved. In [31], by replacing the common one-to-one collision-avoidance with the constructed within-SDC constraints, an optimal control problem whose scale is totally independent of the number of obstacles could be formulated. In [32], combined with the hp method based on the residual error of dynamic constraints, adjusting the number of collocation points and subintervals can improve convergence speed and computational efficiency. In future research, multiple obstacles and multiple types of obstacle models should be considered, and the accuracy of trajectory planning problems can be improved by refining the mesh.

## Acknowledgments

This research was funded by the National Natural Science Foundation of China under Grant U2006228, 52171313, 51839004, and in part by the Key Laboratory Foundation of Underwater Robot Technology under Grant 6142215200305.

## Conflict of interest

The authors declare there is no conflict of interest.

## References

1. T. O. Fossum, G. M. Fragoso, E. J. Davies, J. E. Ullgren, R. Mendes, G. Johnsen, et al., Toward adaptive robotic sampling of phytoplankton in the coastal ocean, *Sci. Robot.*, **4** (2019). <https://doi.org/10.1126/scirobotics.aav3041>
2. F. Chai, K. S. Johnson, H. Claustre, X. Xing, Y. Wang, E. Boss, et al., Monitoring ocean biogeochemistry with autonomous platforms, *Nat. Rev. Earth Environ.*, **1** (2020), 315–326. <https://doi.org/10.1038/s43017-020-0053-y>
3. Y. Tan, J. Wang, J. Liu, Y. Zhang, Unmanned systems security: Models, challenges and future directions, *IEEE Network*, **34** (2020), 291–297. <https://doi.org/10.1109/MNET.001.1900546>

4. J. Teague, M. J. Allen, T. B. Scott, The potential of low-cost ROV for use in deep-sea mineral, ore prospecting and monitoring, *Ocean Eng.*, **147** (2018), 333–339. <https://doi.org/10.1016/j.oceaneng.2017.10.046>
5. H. R. Karimi, Y. Lu, Guidance and control methodologies for marine vehicles: A survey, *Control Eng. Pract.*, **111** (2021). <https://doi.org/10.1016/j.conengprac.2021.104785>
6. X. Wang, J. Liu, X. Su, H. Peng, X. Zhao, C. Lu, A review on carrier aircraft dispatch path planning and control on deck, *Chinese J. Aeronaut.*, **33** (2020), 3039–3057. <https://doi.org/10.1016/j.cja.2020.06.020>
7. X. Wang, J. Liu, H. Peng, X. Qie, X. Zhao, C. Lu, A simultaneous planning and control method integrating APF and MPC to solve autonomous navigation for USVs in unknown environments, *J. Intell. Robot. Syst.*, **105** (2022). <https://doi.org/10.1007/s10846-022-01663-8>
8. Y. Wu, N. Hu, X. Qu, A general trajectory optimization method for aircraft taxiing on flight deck of carrier, *P. I. Mech. Eng. G-J. Aer.*, **233** (2019). <https://doi.org/10.1177/0954410017752224>
9. Y. Ren, J. Wang, X. Zhang, Research on AUV path planning based on multi-factor improved A\* algorithm, *Ship Sci. Tech.*, **44** (2022), 58–62. <http://dx.chinadoi.cn/10.3404/j.issn.1672-7649.2022.11.012>
10. Y. Liu, J. Xiang, S. Cao, AUV path planning based on improved ant colony algorithm, *Comput. Eng. Sci.*, **44** (2022), 536–544. <https://doi.org/10.3969/j.issn.1007-130X.2022.03.021>
11. Z. Chu, F. Wang, T. Lei, C. Luo, Path planning based on deep reinforcement learning for autonomous underwater vehicles under ocean current disturbance, *IEEE Trans. Intell. Vehicles*, **8** (2023), 108–120. <https://doi.org/10.1109/TIV.2022.3153352>
12. L. Zhang, P. Ge, Trajectory optimization and orbit design of spacecraft in hovering mission, *J. Astronaut. Sci.*, **67** (2020), 44–1373. <https://doi.org/10.1007/s40295-020-00226-z>
13. H. Li, Trajectory planning method for manipulator of tunnel trolley based on gauss pseudospectral method, *Constr. Mach. Technol. Manage.*, **35** (2022). <https://doi.org/10.13824/j.cnki.cmtm.2022.06.029>
14. H. Chen, L. Guo, X. Gong, B. Gao, L. Zhang, Automotive control in intelligent era, *Acta Automatica Sinica*, **46** (2020), 1313–1332. <https://doi.org/10.16383/j.aas.c190329>
15. C. Liu, C. Zhang, Multi-stage trajectory optimization of tactical two-stage booster rocket based on gauss pseudospectral method, *Acta Armamentarii*, **40** (2019), 292–302. <https://doi.org/10.3969/j.issn.1000-1093.2019.02.009>
16. Z. Sun, Z. Liu, P. Zhang, Mars entry trajectory quick optimization method for lifting vehicle based on adaptive GPM, *Chinese J. Space Sci.*, **40** (2020), 547–553. <https://doi.org/10.11728/cjss2020.04.547>
17. J. Zhang, S. Zhou, J. Zhao, Z. Shi, Path planning and tracking control for corner overtaking of vehicle based on gauss pseudo-spectral method, *Journal of Tianjin University(Science and Technology)*, **54** (2021), 8. <https://doi.org/10.11784/tdxbz202001041>
18. H. Yao, R. Qi, A research progress of trajectory optimization and guidance for mars lander, *Aerospace Control*, **39** (2021), 3–12. <https://www.doi.org/10.16804/j.cnki.issn1006-3242.2021.04.001>
19. X. Wang, H. Peng, S. Zhang, B. Chen, W. Zhong, A symplectic pseudospectral method for nonlinear optimal control problem with inequality constraints, *ISA Trans.*, **68** (2017), 335–352. <https://www.doi.org/10.1016/j.isatra.2017.02.018>



20. X. Wang, J. Liu, H. Peng, X. Zhao, An iterative framework to solve nonlinear optimal control with proportional delay using successive convexification and symplectic multi-interval pseudospectral scheme, *Appl. Math. Comput.*, **435** (2022), 127448. <https://www.doi.org/10.1016/J.AMC.2022.127448>
21. J. Huang, Z. Liu, Z. Liu, Q. Wang, Pseudo-spectral method for optimal control problem: theory and application, *Electron. Optics Control*, **27** (2020), 63–70. <http://dx.chinadoi.cn/10.3969/j.issn.1671-637X.2020.06.013>
22. W. Xu, J. Jiang, S. Jiang, Y. Zheng, Scale optimization of wings in the climbing section of a near-space morphing hypersonic aircraft, *J. Harbin Eng. Univer.*, **40** (2019), 1134–1141. <https://www.doi.org/10.11990/jheu.201803082>
23. H. Mai, Convergence for the optimal control problems using collocation at Legendre-Gauss points, *Trans. Institute Meas. Control*, **44** (2022), 1263–1274. <https://www.doi.org/10.1177/01423312211043335>
24. W. Qu, H. Zhang, L. Wu, Y. You, Y. Dong, The trajectory design on the captive flight test of booster rocket and the combined-cycled aircraft based on segmented gaussian pseudo-spectral method, *Aerospace Control*, **39** (2021), 28–35. <https://www.doi.org/10.3969/j.issn.1006-3242.2021.04.004>
25. D. Ma, S. Hao, W. Ma, H. Zheng, X. Xu, An optimal control-based path planning method for unmanned surface vehicles in complex environments, *Ocean Eng.*, **245** (2022), 110532. <https://doi.org/10.1016/j.oceaneng.2022.110532>
26. Y. Tang, J. Huang, M. Li, Q. Liu, B. Chen, Multistage iterative optimization strategy for gliding trajectory based on pseudo-spectral method, *Computer Meas. Control*, **27** (2019) 157–162. <http://doi.org/10.16526/j.cnki.11-4762/tp.2019.11.034>
27. L. Ma, W. Cui, Path following control of autonomous underwater vehicle based upon fuzzy hybrid control, *Control Theory Appl.*, **03** (2006), 341–346. <https://www.doi.org/10.3969/j.issn.1000-8152.2006.03.003>
28. Y. Li, X. Li, S. Liu, P. Kang, Application of gauss pseudo-spectral method in trajectory optimization of variable trust missile, *Modern Defense Tech.*, **47** (2019), 71–77. <https://www.doi.org/10.3969/j.issn.1009-086x.2019.03.11>
29. Y. Zhang, W. Zhang, J. Chen, L. Shen, Air-to-ground weapon delivery trajectory planning for UCAVs using Gauss pseudo-spectral method, *Acta Aeronautica et Astronautica Sinica*, **32** (2011), 1240–1251.
30. Y. Liu, X. Zhang, Y. Zhang, X. Guan, Collision free 4D path planning for multiple UAVs based on spatial refined voting mechanism and PSO approach, *Chinese J. Aeronautics*, **32** (2019), 1504–1519. <https://www.doi.org/10.1016/j.cja.2019.03.026>
31. X. Wang, B. Li, X. Su, H. Peng, L. Wang, C. Lu, et al., Autonomous dispatch trajectory planning on flight deck: A search-resampling-optimization framework, *Eng. Appl. Artif. Intell.*, **119** (2023), 105792. <https://doi.org/10.1016/j.engappai.2022.105792>
32. H. Peng, X. Wang, M. Li, B. Chen, An hp symplectic pseudospectral method for nonlinear optimal control, *Commun. Nonlinear Sci.*, **42** (2017), 623–644. <https://doi.org/10.1016/j.cnsns.2016.06.023>

---

**Supplementary**


---



---

**Nomenclatures**


---

$p_x$	The position of AUV in the x direction
$p_y$	The position of AUV in the y direction
$\psi$	The direction angle of the AUV
$v_x$	The velocity of AUV in the x direction
$v_y$	The velocity of AUV in the y direction
$r_z$	The angular velocity of the AUV
$T_u$	Thrust of propeller in the x direction
$T_v$	Thrust of propeller in the y direction
$T_r$	Torque generated by thrust
$m$	Mass of the AUV
$I_z$	The moment of inertia
$X_u$	Additional mass coefficient in the u direction
$X_u$	Linear resistance coefficient in the u direction
$X_{ u  \cdot u}$	Secondary resistance coefficient in the u direction
$Y_v$	Additional mass coefficient in the v direction
$Y_v$	Linear resistance coefficient in the v direction
$Y_{ v  \cdot v}$	Secondary resistance coefficient in the v direction
$N_r$	Additional rotational inertia in r direction
$N_r$	Linear resistance coefficient in the r direction
$N_{ r  \cdot r}$	Secondary resistance coefficient in the r direction
$R(x, y)$	The center of gravity of the AUV
$l_1$	The distance from the center of gravity to the head of the AUV
$l_2$	The distance from the center of gravity to the tail of the AUV
$d$	The width of AUV
$r_x$	The scale coefficients in the x direction
$r_y$	The scale coefficients in the y direction
$(a, b)$	The center position of the graph
$x(t)$	The state variable
$u(t)$	The control variable
$\Phi$	The Mayer form of the objective function
$L$	The Lagrange form of the objective function
$C$	The path constraint function
$\phi$	The boundary constraint function
$\tau$	The time variable
$t_0$	The Initial time
$t_f$	The terminal time
$Li(\tau)$	The interpolation basis function
$D$	The differential approximation matrix
$\omega_k$	The Gauss weight
$x_i^t$	The position of the i-th particle at the t-th iteration

---

*Continue to next page*

---

**Nomenclatures**

---

$v_i^t$	The velocity of the i-th particle at the t-th iteration
$c_1$	The learning factor
$c_2$	The learning factor
$\omega$	The inertia weight
$r$	A random number between (0,1)
$p_g$	The Group optimal value

---

**AIMS Press**

©2023 the Author(s), licensee AIMS Press. This is an open access article distributed under the terms of the Creative Commons Attribution License (<http://creativecommons.org/licenses/by/4.0>)